Mohamed Amri, Philippe Basset, Dimitri Galayko, Francesco Cottone, Einar Halvorsen, S. Duy Nguyen, Fehmi Najar*, and Tarik Bourouina

Stiffness control of a nonlinear mechanical folded beam for wideband vibration energy harvesters

Steifigkeitskontrolle eines nichtlinearen mechanischen gefalteten Strahls für Breitbandvibrations-Erntemaschinen

https://doi.org/10.1515/teme-2017-0087
Received July 12, 2017; accepted May 21, 2018

Abstract: This paper presents a novel approach to design and optimize geometric nonlinear springs for wideband vibration energy harvesting. To this end, we designed a spring with several folds to increase its geometric nonlinearities. A numerical analysis is performed using the Finite Element Method to estimate its quadratic and cubic spring stiffness. A nonlinear effective spring constant is then calculated for different values of the main folding angle. We demonstrate that this angle can increase nonlinearities within the structure resulting in higher bandwidths, and that it is possible to control the behavior of the system to have softening-type or hardening-type response depending on the choice of the folding angle. Based on the Lindstedt-Poincaré perturbation technique, a first order approximation is determined to predict the frequency-response of the system. In order to validate the perturbation analysis, numerical solutions based on long-time integration method and mixed VHDL-AMS/Spice simulations are presented. Finally, this method is applied to a previously published device and shows a good agreement with experiments.

Keywords: Energy harvesting, nonlinear response, frequency response curve, perturbation method.

Zusammenfassung: Dieser Artikel präsentiert einen neuartigen Ansatz zum Entwurf und zur Optimierung geometrischer nichtlinearer Federn für die Energiegewinnung durch Breitbandvibrationen. Zu diesem Zweck verwenden wir ein gefaltetes Balkendesign. Wir fügen einen Faltungswinkel im Hauptstrahl hinzu, um seine geometrischen Nichtlinearitäten zu erhöhen. Eine numerische Analyse wird unter Verwendung der Finite-Elemente-Methode durchgeführt, um ihre quadratische und kubische Federsteifigkeit abzuschätzen. Eine nichtlineare effektive Federkonstante wird dann für verschiedene Werte des Faltwinkels berechnet. Wir zeigen, dass dieser Winkel Nichtlinearitäten innerhalb der Struktur erhöhen kann, was zu höheren Bandbreiten führt, und dass es möglich ist, das Verhalten des Systems so zu steuern, dass je nach Wahl des Faltwinkels eine Antwort vom Erweichungstyp oder vom Härtungstyp erhalten wird. Basierend auf der Lindstedt-Poincaré-Störungstechnik wird eine Näherung erster Ordnung zur Vorhersage der Frequenzantwort des Systems bestimmt. Um die Störungsanalyse zu validieren, werden numerische Lösungen basierend auf der Langzeit-Integrationsmethode und gemischten VHDL-AMS/Spice-Simulationen vorgestellt. Schließlich wird diese Methode auf ein zuvor veröffentlichtes Gerät angewendet und zeigt eine gute Übereinstimmung mit Experimenten.

Schlagwörter: Energy Harvesting, nichtlineare Antwort, Frequenzantwortkurve, Perturbations-Methode.

***Corresponding author: Fehmi Najar,** LASMAP,Tunisia Polytechnic School, University of Carthage, La Marsa, Tunisia, e-mail: fehmi.najar@ept.rnu.tn
Mohamed Amri, LASMAP,Tunisia Polytechnic School, University of Carthage, La Marsa, Tunisia; and Université Paris-Est, ESYCOM, ESIEE Paris, Noisy-le-Grand, France
Philippe Basset, Francesco Cottone, Tarik Bourouina, Université Paris-Est, ESYCOM, ESIEE Paris, Noisy-le-Grand, France
Dimitri Galayko, LIP6, UPMC Universités Paris Sorbonne, Paris, France
Einar Halvorsen, S. Duy Nguyen, University of South-Eastern Norway, Horten, Norway

1 Introduction

The use of environmental vibrations as a source of energy to feed autonomous systems was demonstrated by many researchers in the last decade. However, the vibrations coming from the surrounding environment are not controllable; moreover, they are often non-harmonic, random and broadband. In this framework, the use of linear-like response energy harvester with narrow frequency band, are not appropriate even if these transducers propose high electromechanical coupling coefficients. The idea behind introducing nonlinear energy-harvester is to overcome this drawback by increasing the bandwidth of the system in

terms of mechanical response and thus allowing a better energy conversion for the case of wideband or variable vibration sources.

Several mechanisms can be used to introduce nonlinearities in energy harvester. The nonlinearity could have, in general, one of the following origins: geometrical [1], material [2, 3] or boundary conditions (force [4] or displacement [5]). Other kind of nonlinearities could also be found in multiphysical systems such as piezoaeroelastic energy harvesters [6] or nonlinear electronic interfaces [7]. Despite the source of nonlinearity, the nonlinear behavior describing these energy harvesters can be categorized into two basic mechanisms: monostable [2] and bistable systems [8]. The second category is characterized by what is known as snap through solutions that can exhibit large amplitude of motion and thus generates more energy. However, the control of this kind of systems is complicated [4] and subject to high sensitivity to initial condition. Therefore, the use of monostable systems is, in this regards, more reliable. Other kind of nonlinearity can be taken into account such as fractional damping that induced chaotic response as demonstrated by Cao et al. [9]. Fractional order physical properties have been used also by Kwuimy et al. [10] to different kind of energy harvesters. On the other hand, cubic nonlinear damping using delayed feedback velocity has been introduced by [11] to improve the response of a generic energy harvesting system.

Using bistable systems, many research groups have attempted to enable collecting energy from non-harmonic vibrations and random vibrations. For instance, Cottone et al. [1, 4] proposed to use bistability in order to collect energy efficiently. It was achieved by combining two opposite magnets and a piezoelectric inverted pendulum. Under appropriate conditions, the nonlinear device was able to harvest 6 times more energy than a linear one. Similar approaches have been proposed by Erturk et al. [8] and Stanton et al. [12]. In the absence of external magnetic forces, buckled beams can also be used to generate dynamical bistabilities, using piezoelectric [13, 14] or electromagnetic [15] transduction.

For monostable systems, the nonlinearity is, in most of the cases, due to large displacements. Which is very common in microsystems because of scale effect. Vibration Energy Harvester (VEH) are also subject to this kind of nonlinearity. This nonlinearity is in general of the Duffing type [16]. It leads to possibly large bandwidth. However, increasing the bandwidth in this case will be toward high frequencies because of cubic positive nonlinearity, which is undesirable for microscale VEH because its natural frequencies are already high due to scale effect and ambient vibrations tend to be low. Next we present some of the recently proposed similar designs and their respective essential findings.

Hajati and Kim [17] designed a clamped-clamped MEMS piezoelectric VEH allowing wide-bandwidth with Duffing-type resonance. They showed that a power density of $2\,\mu W/cm^3$ could be achieved. Using an electromagnetic energy harvester with Duffing-type nonlinearity, Green et al. [16] tested its performance when subjected to a broadband white noise base acceleration. They showed analytically and experimentally that the optimum load is different to the one calculated by impedance matching. Incorporating a stop-end to their flexible structure with interdigitated electrodes, Basset et al. [18] designed an electrostatic energy harvester working over the range of 140 to 160 Hz and producing more than $2\,\mu W$. The nonlinear electromechanical coupling due to the presence of the electrostatic force was modeled by Mahmoud et al. [19] for an interdigitated VEH design. They proposed design rules for realizing wideband electrostatic VEHs, and developed closed-form formulae for the extracted power under moderately large excitations.

Under the monostable system behavior, other research groups proposed the use of deliberately nonlinear structure that exhibit nonlinearity even at relatively low displacements. Marzencki et al. [20] presented a nonlinear MEMS VEH based on clamped-clamped piezoelectric beam leading to a hardening-type behavior due to midplane stretching. Miki et al. [21] fabricated a micro electret generator based on nonlinear springs made of parylen. Nguyen [22, 23] used asymmetric, effectively softening springs, to harvest energy under colored noise excitations. Tvedt et al. [5] presented an electrostatic VEH that can have both hardening and softening behavior depending on the excitation levels: the hardening-type behavior of four cantilever-guided beam was achieved thanks to large displacements. However, the observed softening-type response was attributed to the stresses due to packaging without validation. Soliman et al. [24] and Phu and Halvorsen [25] used piecewise oscillators with a hardening behavior induced by impacts with stoppers to increase the bandwidth. The same idea was used by Stoykov et al for a piezoelectric energy harvester [26] and by Borowiec et al. [27] with an electromagnetic transduction mechanism. A softening behavior has been obtained thanks to electrostatic nonlinearities and mechanical stoppers by Guillemet et al. [28] and Cottone et al. [29].

In this work, we present a strategy to analyze the design parameters of a nonlinear springs with cubic and quadratic nonlinearities that can provide either softening-type or hardening-type behaviors. The objective is to develop an analytical tool that generates easily the non-

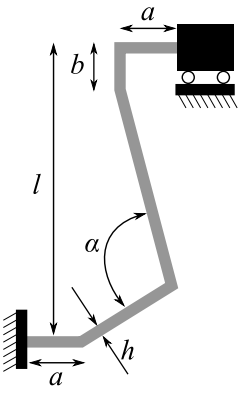

Figure 1: Layout of the proposed nonlinear spring to be used for energy harvesting application.

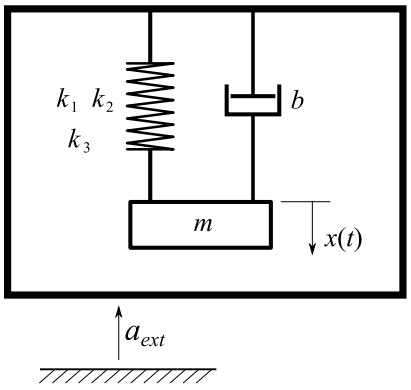

Figure 2: Simplified dynamical model of the vibration-driven energy harvester including the nonlinear spring.

linear dynamic response for different design parameters of the nonlinear spring. An angle α is introduced in the main beam of a crab-leg flexure. Depending on the angle value, the spring can have either hardening or softening behavior. This paper is organized as follows. In subsection 2.1, we present the design of the nonlinear spring and the lumped model of the energy harvester. A numerical stiffness analysis is presented in subsection 2.2 and the frequency-response of the system is analyzed in subsection 2.3. In section 3, we compare experimental measurements from [22] with the numerical analysis presented in section 2.

2 Mechanical spring design and analysis

In this section, we analyze the introduction of an angle α in the main spring beam of a crab-leg flexure (Figure 1). Firstly, we present the simplified dynamical model of the nonlinear oscillator. A third order Taylor series expansion is used in order to approximate the spring restoring force as a function of the displacement. Then, the spring constants are evaluated using Finite Element Method (FEM). Finally, we use the Lindstedt-Poincaré Perturbation Technique (LPPT) to evaluate the frequency-response of the system. For the best of our knowledge, this is the first time the LPPT is used for this kind of systems.

2.1 Dynamical model

The studied vibration-driven energy harvester consists of an inertial mass m, a nonlinear spring and a mechanical damper b (Figure 2). The nonlinear spring's restoring force F_R is defined by its constants k_1, k_2 and k_3 in the displacement x by:

$$F_R = -(k_1 x + k_2 x^2 + k_3 x^3) \tag{1}$$

We consider that the oscillator as a single degree of freedom lumped system. When the rigid frame vibrates with acceleration a_{ext}, the mass moves with respect to the rigid frame; producing a relative displacement $x(t)$. As an example for this analysis, we use typical dimensions and design rules based on the MEMS VEH described in [30]. The inertial mass is 1 cm×1 cm×380 μm in dimensions. We assume that viscous-air damping is the predominant energy dissipation mechanism in the structure and that it is linear, i. e., the mechanical damping force is proportional to the velocity and the total damping force F_D can be written as follows

$$F_D = -b\dot{x} \tag{2}$$

where the over dot designate derivative with respect to time.

Newton's second law gives the equation of motion of the nonlinear oscillator. It is written as

$$F_R + F_D + F_{ext} = m\ddot{x} \tag{3}$$

where $F_{ext} = -ma_{ext}$ is the inertial force term.

2.2 Numerical spring constant analysis

Each segment of the spring (Figure 1) is 30 μm in width and 380 μm in thickness. The total length of the spring is l = 2 mm. In case of large displacements, the spring force F_R is not proportional to x due to geometric nonlinearities. So, we take a third order Taylor's series expansion of the nonlinear restoring force given by Equation (1) where k_1 is

the normal linear spring constant, k_2 and k_3 are the second and the third order corrections, respectively. Those constants depend on spring dimensions, geometric parameters α and a, and the boundary conditions.

An FEM commercial package (ANSYS) is used to determine the displacement-force curves for different angles α and a. The length b is 100 μm. This segment helps to keep a low stiffness in the spring while having nonlinear behavior. Each beam segment is modeled by 40 elements. A horizontal displacement is applied on the guided-end gradually. The value of spring force is then determined for each load increment. The force-displacement curve is plotted in Figure 3 for a set of angles and for a = 100 μm. The curves are asymmetric due to the asymmetry of the spring geometry and orientation. It can be seen that the curves are linear only for small displacements.

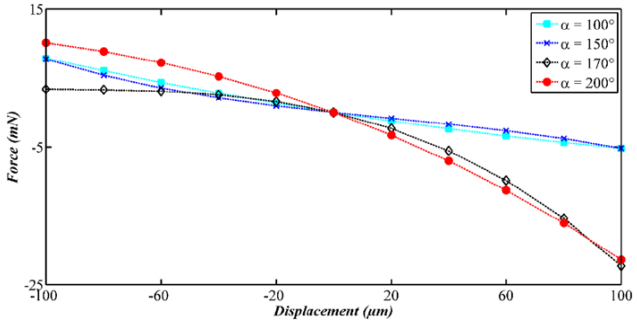

Figure 3: Force-displacement curves of the nonlinear spring obtained by FEM for various values of α, a = 100 μm.

The spring constants k_1, k_2 and k_3 are numerically evaluated using the following optimization formulation based on the Least Square Method [31]:

$$\min_{k_1,k_2,k_3} \sum_{i=1}^{m} \left(F_{Ri} - \left(k_1 x_i + k_2 x_i^2 + k_3 x_i^3\right)\right)^2 \qquad (4)$$

where x_i is the displacement from the equilibrium position and F_{Ri} is the restoring force at displacement i. The objective of this method is to find the best (k_1, k_2, k_3) that minimize the quadratic error for each angle. Figure 3 shows the FEM points (with markers) versus the cubic approximations (dashed lines) for α = 100°, 150°, 170° and 200°. An excellent agreement with absolute error less than 1 % is observed.

The obtained fitted spring constants to the FEM results are shown in Figures 4. It can be seen that all the curves are asymmetric because of the asymmetry of the spring. In addition, the most significant region is observed for α between 140° and 200°. The linear spring stiffness k_1

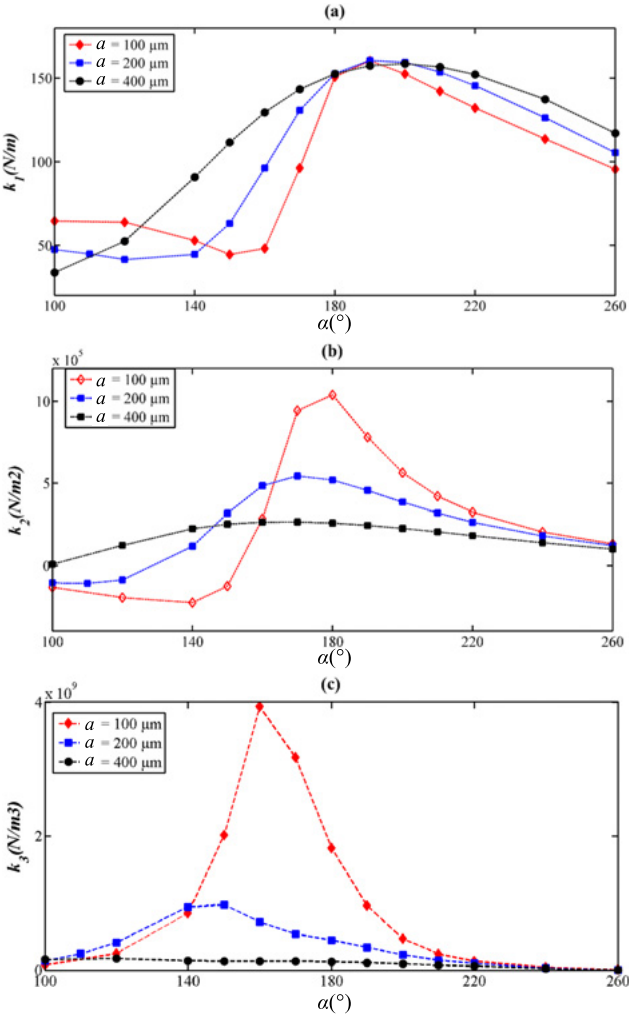

Figure 4: Linear and nonlinear spring constants for the proposed nonlinear spring design obtained from Finite Elements Method for different values of a and α. (a): k_1, (b): k_2; (c): k_3.

is maximum around α = 190° while the highest levels of quadratic and cubic nonlinearities correspond to α = 180° and α = 160°, respectively. One can observe that for high values of a, the cubic nonlinearity is relatively weak. It also can be seen that the angle α can lower the value of linear spring constant k_1. Finally, it is interesting to note that the range where α generates higher cubic nonlinearity corresponds also to a lower linear stiffness inducing a lower natural frequency. This is suitable to energy harvesting applications where low frequency and large bandwidth are sought.

2.3 Frequency response

To study the effect of the spring nonlinearities on the bandwidth of a VEH, we will now determine the frequency-

response of the system using perturbation analysis. To limit rotational modes, the 1 cm^2 silicon mass is suspended by 4 identical nonlinear springs. The equation of motion can be written out as

$$m\ddot{x} + b\dot{x} + \hat{k}_1 x + \hat{k}_2 x^2 + \hat{k}_3 x^3 = -ma_{ext} \tag{5}$$

where $(\hat{k}_1, \hat{k}_2, \hat{k}_3)$ are the equivalent spring constants: $(\hat{k}_1, \hat{k}_2, \hat{k}_3) = 4 \times (k_1, k_2, k_3)$. In the following, for convenience, we will drop the hats from the equivalent spring constants. Equation (5) contains cubic and quadratic nonlinearities. Several possible perturbation techniques can be applied in order to determine an analytical approximation of the frequency-response for nonlinear oscillations. Some methods are based on the nonlinear expansion of the amplitude like the straightforward expansion approach. But those methods are doomed to fail because they do not take into account that the resonant frequency becomes a function of the oscillation amplitude [32]. In this paper, we analyze the dynamics of the system by using the Lindstedt-Poincaré Perturbation Technique (LPPT) which gives a similar result as the Method of Renormalization, but with less algebra [32]. In order to validate the perturbation approach, numerical solutions given by Long-Time Integration method using a Runge-Kutta scheme and VHDL-AMS simulations are also presented.

2.3.1 Lindstedt-Poincaré perturbation technique

The fundamental idea of the LPPT is the observation that the nonlinearities alter the resonance frequency of the system from the linear one $\omega_0 = \sqrt{\frac{k_1}{m}}$ to $\omega_0'(\epsilon)$, where ϵ is the perturbation parameter [33]. Far from resonance, the nonlinearities can be neglected and the time harmonic linear vibration amplitude $X(\omega)$ can be written as

$$X(\omega) = \frac{a_{ext}(\omega)}{\sqrt{(\omega^2 - {\omega_0}^2)^2 + (\frac{\omega\omega_0}{Q})^2}} \tag{6}$$

where $Q = \omega_0 \frac{m}{b}$ denotes the linear quality factor and ω the excitation frequency.

Near resonance, the frequency-response can be approximated using the LPPT. We first consider unforced-undamped vibration problem given by:

$$m\ddot{x} + k_1 x + k_2 x^2 + k_3 x^3 = 0 \tag{7}$$

We introduce the perturbation parameter ϵ and assume that the nonlinear terms in Equation (7) will change the resonance frequency to $\omega_0'(\epsilon)$, we introduce the following transformations [34]:

$$\tau = t\omega_0', \quad k_2 = \epsilon\lambda m, \text{ and } k_3 = \epsilon^2\gamma m \tag{8}$$

Also we assume that x and ω_0' can be expanded in powers of ϵ:

$$\begin{cases} x = x_0 + \varepsilon x_1 + \varepsilon^2 x_2 + \ldots \\ {\omega_0}' = \omega_0 + \varepsilon\omega_1 + \varepsilon^2\omega_2 + \ldots \end{cases} \tag{9}$$

Substituting Equations (9) and (16) into Equation (7), expanding the results and keeping only terms to $O(\epsilon^3)$, equating the coefficients of like powers of ϵ to zero yields:

$$\omega_0^2 x_{0,\tau\tau} + \omega_0^2 x_0 = 0 \tag{10}$$

$$\omega_0^2 x_{1,\tau\tau} + \omega_0^2 x_1 = -\lambda x_0^2 - 2\omega_0\omega_1 x_{0,\tau\tau} \tag{11}$$

$$\omega_0^2 x_{2,\tau\tau} + \omega_0^2 x_2 = -\lambda x_0 x_1 - \gamma x_0^3 - (2\omega_0\omega_2 + \omega_1^2) x_{0,\tau\tau} - 2\omega_0\omega_1 x_{1,\tau\tau} \tag{12}$$

The solution of Equation (10) can be expressed as

$$x_0 = X\cos\tau \tag{13}$$

Replacing Equation (13) into (11) and requesting that secular terms should be eliminated, yields the condition $\omega_1 = 0$. Therefore, the solution of Equation (11) is given by

$$x_1 = \frac{\lambda X^2}{\omega_0^2}\left(-\frac{1}{2} + \frac{1}{6}\cos 2\tau\right) \tag{14}$$

Now using Equation (14) and (13) into (12), eliminating the secular terms leads to

$$\omega_2 = \left(\frac{3}{8}\gamma - \frac{5}{12}\frac{\lambda^2}{\omega_0^2}\right)\frac{X^2}{\omega_0} \tag{15}$$

Recalling that ${\omega_0}' = \omega_0 + \varepsilon^2\omega_2 + O(\epsilon^3)$, and using Equation (8) we end up with ${\omega_0}' = \omega_0 + \kappa X^2$, where κ denotes the effective nonlinear spring constant that measures the change of the resonance frequency, it is given by:

$$\kappa = \frac{3k_3}{8k_1}\omega_0 - \frac{5{k_2}^2}{12{k_1}^2}\omega_0 \tag{16}$$

Figure 5 illustrates the obtained results for κ. It can be seen that when a increases, the nonlinearity decreases and the nonlinearities become very small when a exceeds 400 μm. For $a = 100$ μm, the best angle that maximizes nonlinearities is $\alpha = 170^\circ$.

Figure 6 shows the first harmonic of the frequency-response for an oscillator with $a = 100$ μm under sinusoidal excitations for different values of α. The input acceleration amplitude is 1 g. All curves are normalized with respect to the frequency and amplitude corresponding to $\alpha =$

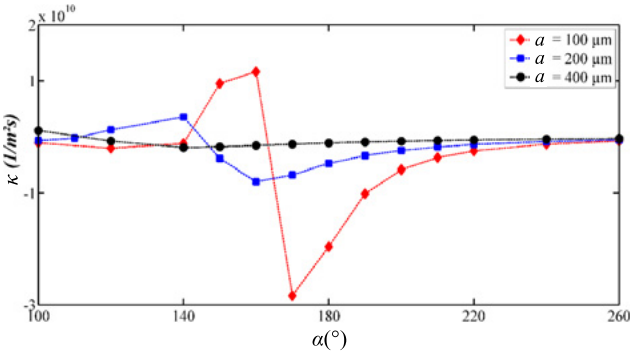

Figure 5: Variation of the effective nonlinear spring constant κ, obtained by LPPT, versus α the folding angle of the spring, for several value of a.

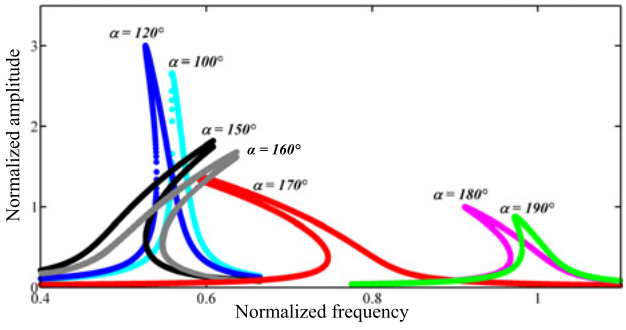

Figure 6: Normalized frequency-response curves of the system under harmonic excitation using LPPT, 1 g acceleration amplitude, for various values of α (a = 100 µm, normalization is done with respect to the response when α = 180°).

180°. The largest bandwidth is associated with the highest value of the nonlinear spring constant κ, i. e. α = 170°.

It is interesting to note that the frequency-response curve of different angle α can be lower or higher the frequency-response curve of the straight spring configuration, e. g. α = 180°. In addition, by varying the angle α, both softening and hardening behaviors are obtained. This is explained by the presence of quadratic and cubic nonlinearities in the spring restoring force expression. Three scenarios are possible, depending on the sign of:

1. If the impact of quadratic stiffness neutralize the effect of the positive cubic stiffness $\left(\frac{3k_3}{8k_1} \approx \frac{5{k_2}^2}{12{k_1}^2}\right)$. In this case, the oscillator behaves linearly; which is the case for α = 100°.
2. If the impact of cubic stiffness is stronger than the one of quadratic stiffness $\left(\frac{3k_3}{8k_1} > \frac{5{k_2}^2}{12{k_1}^2}\right)$, becomes strictly positive and the system will have the hardening-type behavior; which is the case of α = 150° or 160° for instance.

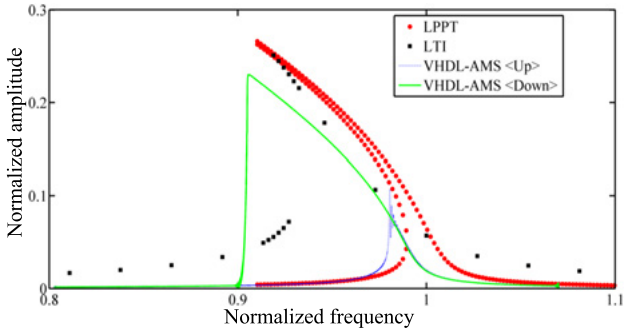

Figure 7: Comparison between the frequency-response curves of the system obtained by VHDL-AMS, LTI and LPPT (α = 170°, Q = 50, a_{ext} = 0.5 g).

3. If the influence of cubic stiffness is weaker than the one of quadratic stiffness $\left(\frac{3k_3}{8k_1} < \frac{5{k_2}^2}{12{k_1}^2}\right)$, becomes strictly negative and the system will have a softening-type behavior; which is the case of α = 170° or 180°.

In order to validate the perturbation analysis, Long-Time Integration (LTI) Method and mixed VHDL-AMS/Spice simulations are performed. In fact, VHDL-AMS is an industry standard (IEEE standard 1076-1993 and IEEE Std. 1076.1-1999) hardware description language used to model mixed signal circuits, it is combined here with SPICE, the famous electronic circuit simulator. These tools are used in general in the microelectronic industry to model mixed electric/non-electric designs. The LTI method consists of integrating Equation (5) numerically for a long time using the Runge-Kutta method. This method can only locate stable solutions. In addition, the simplified dynamical model of the energy harvester is implemented using VHDL-AMS. Then, this model is included in an Eldo circuit and the whole problem is simulated using ADVanceMS simulator for both direct and reverse frequency sweeps [35]. Figure 7 shows the frequency-response of the system given by the three techniques. The results are very similar for the different approaches. However, a difference is observed for high displacement. This can be explained by the fact that we considered only the first harmonic when we used the LPPT.

3 Experimental study

3.1 Description of the device

In this section, we apply the previous methodology on an in-plane overlap electrostatic-VEH (e-VEH) developed previously in [22].

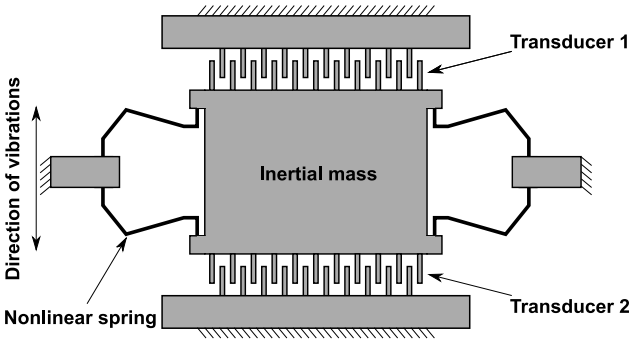

Figure 8: Schematic view of a MEMS in-plane overlap e-VEH with four nonlinear springs used as suspensions of the inertial mass.

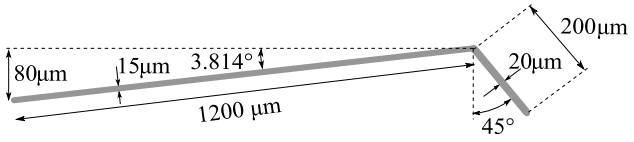

Figure 9: Geometry and dimensions of the nonlinear folded spring.

Figure 8 presents a schematic view of a MEMS in-plane overlap energy harvester. It is made of a silicon inertial mass m = 35.25 mg suspended by four angled springs and two electrostatic transducers to extract the mechanical energy of the harvester and convert it into electric energy. A full description of the device can be found in [22]. Next, the lumped model of the energy harvester is presented and a comparison between the LPPT and the LTI solutions is presented.

3.2 The nonlinear spring force

Figure 9 shows a schematic view of the angled spring. Nonlinearities are achieved through the angle introduced in the main beam. Figure 10 shows the force-displacement curve obtained from FEM analysis. One can see that the response of the angled spring is not symmetric. For this reason, two asymmetrical electromechanical transducers are used to convert a part of the mechanical energy into electrical form. A third order approximation is proposed in order to represent the restoring force:

$$F_R = -(k_1 x + k_2 x^2 + k_3 x^3) \tag{17}$$

The obtained coefficients are the following: 4.1147×10^2 N/m, 7.1544×10^6 N/m^2 and 5.6955×10^{10} N/m^3 for k_1, k_2 and k_3 respectively.

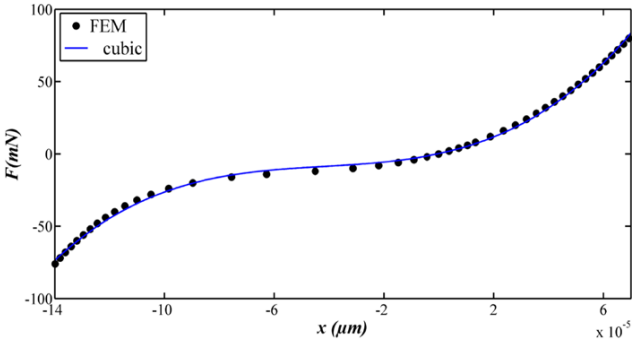

Figure 10: Variation of the force developed by the nonlinear spring as a function of the tip displacement using FEM and compared to a fitted cubic polynomial function.

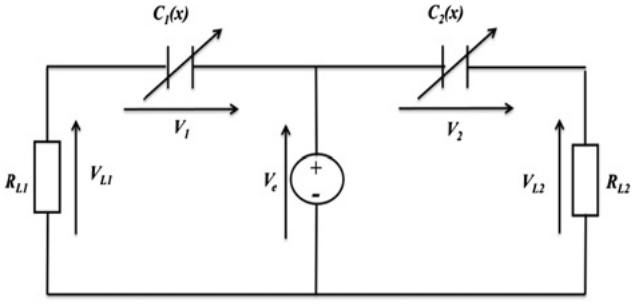

Figure 11: Schematic view of the conditioning circuit to be used with the proposed e-VEH.

3.3 Conditioning circuit

Figure 11 shows the circuit used to extract energy from the VEH. This lumped model is characterized by one mechanical degree of freedom x which represents the mass displacement and two electrical degrees of freedom; the charges $q_1(x)$ and $q_2(x)$ on the variable capacitor electrodes $C_1(x)$ and $C_2(x)$, respectively. The variable capacities corresponds to transducer 1 and 2 in Figure 8.

Let m be the mass of the system. We denote by $F_D = -b\dot{x}$, F_{Elec} and $F_{Ext} = ma_{ext}$ the damping force, the electrical force induced by the transducers and the excitation force, respectively. The differential equations describing the motion of the system and the charge variation in the two capacitors are derived using Newton's second law and Ohm's law as follows:

$$\begin{cases} m\ddot{x} = F_D + F_R + F_{Elec} + F_{Ext} \\ R_{L1}\frac{dq_1}{dt} + \frac{q_1}{C_1(x)} = V_e \\ R_{L2}\frac{dq_2}{dt} + \frac{q_2}{C_2(x)} = V_e \end{cases} \tag{18}$$

where R_{L1} and R_{L2} are the load resistances on the transducers 1 and 2, respectively.

The fingers of the two electrodes are assumed to be rigid and parallel. For $C_1(x)$ and $C_2(x)$ we use the parallel-plate form with an additional parasitic capacitance:

$$\begin{cases} C_1(x) = C_p + \frac{C_{01}}{x_{01}}(x_{01} + x) \\ C_2(x) = C_p + \frac{C_{02}}{x_{02}}(x_{02} - x) \end{cases} \tag{19}$$

where C_p represents the parasitic capacitances in circuit 1 and 2 (which are equal in this case), and C_{01} and C_{02} are the nominal transducer capacitances that depend on the transducer geometry [21]. This form can at least partially account for some fringing field effects if the parameters are obtained numerically or from measurements.

3.4 Simplified dynamical model

For this In-plane Overlap e-VEH with low bias voltage, the electromechanical coupling is very weak. Hence, the electrostatic forces can be ignored and the dimensionless differential equation describing the motion of the inertial mass can be written as:

$$m\ddot{x} + b\dot{x} + k_1 x + k_2 x^2 + k_3 x^3 = -m a_{ext} \tag{20}$$

Figure 12 shows the peak output voltage on one transducer as a function of frequency under the frequency sweep at the peak acceleration amplitude of 0.11 g. The simulation curve is obtained by integrating the simplified equation of motion (Equation (20)) based on Finite Difference Method (FDM). A good agreement can be observed compared to experimental results. Hence, electrical forces will be ignored in the rest of the paper.

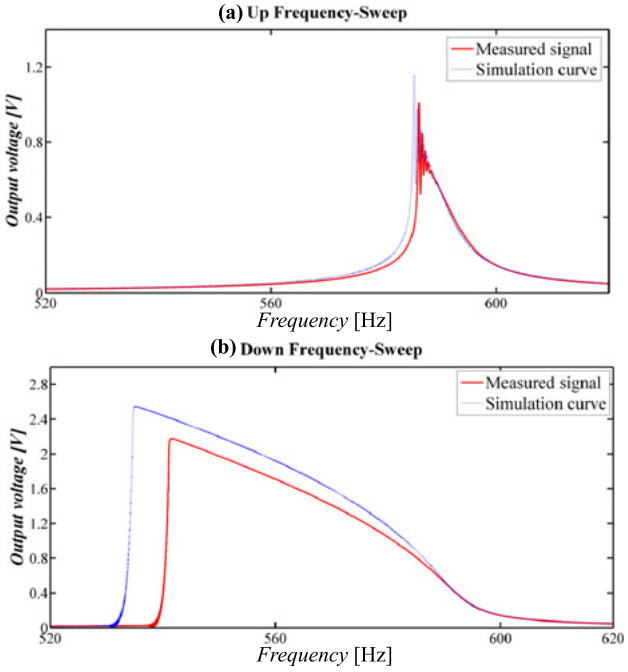

Figure 12: Peak output voltage on transducer 1 versus frequency (chirp rate: 2.667 Hz/s, R_{L1} = 18 Mω, R_{L2} = 17.2 Mω, bias voltage = 24.6 V and maximum peak acceleration amplitude = 0.11 g, Q = 50.

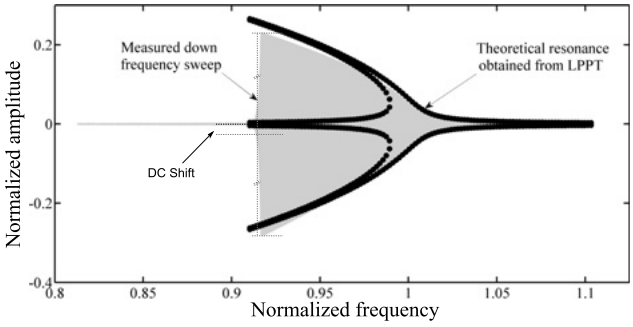

Figure 13: Displacement of the inertial mass versus frequency (frequency rate: 2.667 Hz/s, R_{L1} = 18 Mω, R_{L2} = 17.2 Mω, Bias voltage = 24.6 V and maximum acceleration amplitude = 0.11 g [22]).

3.5 LPPT versus experimental results

In this part, a comparison between the experiments and the perturbation approach is presented. We conclude the displacement x of the proof mass from experimental data using an explicit scheme (Forward Finite Difference Method). To do so, we integrate the following equation where the unknown variable is x:

$$R_{L1}\frac{dq_1}{dt} + \frac{q_1}{C_p + \frac{C_{01}}{x_{01}}(x_{01} + x)} = V_e \tag{21}$$

Using the spring constants obtained from Figure 10, we have found a good agreement between the measured signal and the LPPT in a qualitative point of view. However, the bifurcation points of the curves did not agree. In order to avoid this problem, we have fit the spring constants of the model until the responses agree. The obtained results are shown in Fig. 13. The LPPT curve presents stable and unstable solutions of the first harmonic while experimental curve presents only stable solutions of a reverse frequency sweep cycle. The experimental curve is almost under the envelop of the theoretical resonance obtained from LPPT. The main difference is that the DC shift appearing for high displacement amplitude is not taken into account in the LPPT curve. This is expected because only the first harmonic is considered in the perturbation technique.

4 Conclusion

In this paper, we investigated a new strategy to design and optimize nonlinear springs for wideband VEHs. We were particularly interested in its intrinsic geometric nonlinearities that appear when the structure exhibits large displacements. Those nonlinearities are included to the dynamics of the system thanks to a folded beam design with a folding angle α. FEM analysis was used in order to estimate the behavior of the springs under relatively large displacements. The spring restoring force is then approximated by a third order polynomial function. It appears that α adds both quadratic and cubic nonlinearities to the behavior of the system. A perturbation analysis is performed in order to predict the impact of α on nonlinear oscillations. We used a first order approximation based on the Lindstedt-Poincaré perturbation technique and we analyzed the frequency-response for different values of the angle α. Tuning of the softening and hardening-types behaviors of the nonlinear spring have been obtained by controlling the angle α through the effective stiffness. Numerical solutions based on Long-Time Integration method and VHDL-AMS are performed to valid the perturbation method. The proposed approach is applied to the case of an In-plane Overlap e-VEH with folded beam. A good agreement is observed between experimental measurements and the theoretical results obtained from our perturbation analysis. The proposed design and the accompanying analytical solution, based on the Lindstedt-Poincaré perturbation technique, can be used to improve existing energy harvesting designs where only linear springs have been used.

References

1. R. Masana and M. F. Daqaq, Relative performance of a vibratory energy harvester in mono-and bi-stable potentials, *Journal of Sound and Vibration* 330(24) (2011), 6036–6052.
2. A. Abdelkefi, A. H. Nayfeh and M. R. Hajj, Modeling and analysis of piezoaeroelastic energy harvesters, *Nonlinear Dynamics* 67(2) (2012), 925–939.
3. E. Zaouali, F. Najar and K. Mrabet, Dielectric Elastomer as Active Material in Membranes for Vibration-Based Energy Harvesting, in: *MEDYNA 2013: 1st Euro-Mediterranean Conference on Structural Dynamics and Vibroacoustics, Marrakech, Morocco*.
4. F. Cottone, H. Vocca and L. Gammaitoni, Nonlinear energy harvesting, *Physical Review Letters* 102(8) (2009), 080601.
5. L. G. W. Tvedt, D. S. Nguyen and E. Halvorsen, Nonlinear behavior of an electrostatic energy harvester under wide-and narrowband excitation, *Journal of Microelectromechanical systems* 19(2) (2010), 305–316.
6. A. Abdelkefi, A. H. Nayfeh and M. R. Hajj, Design of piezoaeroelastic energy harvesters, *Nonlinear Dynamics* 68(4) (2012), 519–530.
7. L. Garbuio, M. Lallart, D. Guyomar, C. Richard and D. Audigier, Mechanical energy harvester with ultralow threshold rectification based on SSHI nonlinear technique, *IEEE Transactions on Industrial Electronics* 56(4) (2009), 1048–1056.
8. A. Erturk and D. J. Inman, Broadband piezoelectric power generation on high-energy orbits of the bistable Duffing oscillator with electromechanical coupling, *Journal of Sound and Vibration* 330(10) (2011), 2339–2353.
9. Junyi Cao, Arkadiusz Syta, Grzegorz Litak, Shengxi Zhou, Daniel J. Inman and Yangquan Chen, Regular and chaotic vibration in a piezoelectric energy harvester with fractional damping, *The European Physical Journal Plus* 130(6) (2015), 103.
10. C. A. Kitio Kwuimy, G. Litak and C. Nataraj, Nonlinear analysis of energy harvesting systems with fractional order physical properties, *Nonlinear Dynamics* 80(1–2) (2015), 491–501.
11. A. Bichri, I. Kirrou and M. Belhaq, Energy harvesting of nonlinear damping system under time delayed feedback gain, in: *MATEC Web of Conferences*, vol. 83, EDP Sciences, p. 02002, 2016.
12. S. C. Stanton, C. C. McGehee and B. P. Mann, Nonlinear dynamics for broadband energy harvesting: Investigation of a bistable piezoelectric inertial generator, *Physica D: Nonlinear Phenomena* 239(10) (2010), 640–653.
13. F. Cottone, L. Gammaitoni, H. Vocca, M. Ferrari and V. Ferrari, Piezoelectric buckled beams for random vibration energy harvesting, *Smart materials and structures* 21(3) (2012), 035021.
14. W. Q. Liu, A. Badel, F. Formosa, Y. P. Wu and A. Agbossou, Novel piezoelectric bistable oscillator architecture for wideband vibration energy harvesting, *Smart materials and structures* 22(3) (2013), 035013.
15. F. Cottone, P. Basset, H. Vocca, L. Gammaitoni and T. Bourouina, Bistable electromagnetic generator based on buckled beams for vibration energy harvesting, *Journal of Intelligent Material Systems and Structures* 25(12) (2014), 1484–1495.
16. P. L. Green, K. Worden, K. Atallah and N. D. Sims, The benefits of Duffing-type nonlinearities and electrical optimisation of a mono-stable energy harvester under white Gaussian excitations, *Journal of Sound and Vibration* 331(20) (2012), 4504–4517.
17. A. Hajati and S.-G. Kim, Ultra-wide bandwidth piezoelectric energy harvesting, *Applied Physics Letters* 99(8) (2011), 083105.
18. P. Basset, D. Galayko, F. Cottone, R. Guillemet, E. Blokhina, F. Marty and T. Bourouina, Electrostatic vibration energy harvester with combined effect of electrical nonlinearities and mechanical impact, *Journal of Micromechanics and Microengineering* 24(3) (2014), 035001.
19. M. A. E. Mahmoud, E. M. Abdel-Rahman, E. F. El-Saadany and R. R. Mansour, Electromechanical coupling in electrostatic micro-power generators, *Smart Materials and Structures* 19(2) (2010), 025007.
20. M. Marzencki, M. Defosseux and S. Basrour, MEMS vibration energy harvesting devices with passive resonance frequency adaptation capability, *Journal of Microelectromechanical Systems* 18(6) (2009), 1444–1453.

21. D. Miki, M. Honzumi, Y. Suzuki and N. Kasagi, Large-amplitude MEMS electret generator with nonlinear spring, in: *Micro Electro Mechanical Systems (MEMS), 2010 IEEE 23rd International Conference on*, IEEE, pp. 176–179, 2010.
22. D. S. Nguyen, E. Halvorsen, G. U. Jensen and A. Vogl, Fabrication and characterization of a wideband MEMS energy harvester utilizing nonlinear springs, *Journal of Micromechanics and Microengineering* 20(12) (2010), 125009.
23. D. S. Nguyen, E. Halvorsen, G. U. Jensen and A. Vogl, Fabrication and characterization of a wideband MEMS energy harvester utilizing nonlinear springs, *Journal of Micromechanics and Microengineering* 20(12) (2010), 125009.
24. M. S. M. Soliman, E. M. Abdel-Rahman, E. F. El-Saadany and R. R. Mansour, A wideband vibration-based energy harvester, *Journal of Micromechanics and Microengineering* 18(11) (2008), 115021.
25. C. P. Le and E. Halvorsen, MEMS electrostatic energy harvesters with end-stop effects, *Journal of Micromechanics and Microengineering* 22(7) (2012), 074013.
26. S. Stoykov, G. Litak and E. Manoach, Vibration energy harvesting by a Timoshenko beam model and piezoelectric transducer, *The European Physical Journal Special Topics* 224(14–15) (2015), 2755–2770.
27. Marek Borowiec, Grzegorz Litak and Stefano Lenci, Noise effected energy harvesting in a beam with stopper, *International Journal of Structural Stability and Dynamics* 14(08) (2014), 1440020.
28. R. Guilllemet, P. Basset, D. Galayko, F. Cottone, F. Marty and T. Bourouina, Wideband MEMS electrostatic vibration energy harvesters based on gap-closing interdigited combs with a trapezoidal cross section, in: *Micro Electro Mechanical Systems (MEMS), 2013 IEEE 26th International Conference on*, IEEE, pp. 817–820, 2013.
29. F. Cottone, P. Basset, R. Guillemet, D. Galayko, F. Marty and T. Bourouina, Non-linear MEMS electrostatic kinetic energy harvester with a tunable multistable potential for stochastic vibrations, in: *Solid-State Sensors, Actuators and Microsystems (TRANSDUCERS & EUROSENSORS XXVII), 2013 Transducers & Eurosensors XXVII: The 17th International Conference on*, IEEE, pp. 1336–1339, 2013.
30. P. Basset, D. Galayko, A. M. Paracha, F. Marty, A. Dudka and T. Bourouina, A batch-fabricated and electret-free silicon electrostatic vibration energy harvester, *Journal of Micromechanics and Microengineering* 19(11) (2009), 115025.
31. C. L. Lawson and R. J. Hanson, *Solving least squares problems*, 15, Siam, 1995.
32. A. H. Nayfeh, *Introduction to perturbation techniques*, John Wiley & Sons, 2011.
33. V. Kaajakari, T. Mattila, A. Oja and H. Seppa, Nonlinear limits for single-crystal silicon microresonators, *Journal of Microelectromechanical systems* 13(5) (2004), 715–724.
34. A. H. Nayfeh, *Perturbation methods*, John Wiley & Sons, 2008.
35. D. Galayko, R. Pizarro, P. Basset and A. M. Paracha, AMS modeling of controlled switch for design optimization of capacitive vibration energy harvester, in: *Behavioral Modeling and Simulation Workshop, 2007. BMAS 2007. IEEE International*, IEEE, pp. 115–120, 2007.

Bionotes

Mohamed Amri
LASMAP,Tunisia Polytechnic School, University of Carthage, La Marsa, Tunisia
Université Paris-Est, ESYCOM, ESIEE Paris, Noisy-le-Grand, France
amri369@gmail.com

Mohamed Amri is a computational Geomechanics specialist at Excellence Logging with over 5 years of experience in the modeling of Oil & Gas drilling efficiency and vibrations. He received a PhD from the Mining School of Paris in 2016 in the field of Geomechanics. He was a research assistant at ESIEE Paris in 2012 at the ESYCOM laboratory. His main research included the modeling and the optimization of MEMS devices.

Philippe Basset
Université Paris-Est, ESYCOM, ESIEE Paris, Noisy-le-Grand, France
philippe.basset@esiee.fr

Philippe Basset, is professor at Université Paris-Est / ESIEE Paris. He received his Ph.D from IEMN, University of Lille in 2003 in the areas of microelectronic and micro-electro-mechanical-systems (MEMS). In 2004 he was a post-doc at CMU, Pittsburgh, USA and he joined ESIEE Paris in 2005. He is currently deputy director of the ESYCOM laboratory. His current research interests include micro-power sources for autonomous systems and micro/nano-structuration of silicon. He serves in the International Steering Committee of the PowerMEMS conference since 2015.

Dimitri Galayko
LIP6, UPMC Universités Paris Sorbonne, Paris, France
d.galayko@esiee.fr

Dimitri Galayko was graduated from Odessa State Polytechnic University (Ukraine) in 1998, he received his master degree from Institute of Applied Sciences of Lyon (INSA-LYON, France) in 1999. He made his PhD thesis in the Institute of Microelectronics and Nanotechnologies (IEMN, Lille, France) and received the PhD degree from the University Lille-I in 2002. Since 2005 he is an associate professor in University Paris VI (UPMC, Sorbonne Universités) in the Laboratory of Computer Science (LIP6). His research interests cover design and modeling of heterogeneous systems involving a com-

bination of classical CMOS integrated circuit with physical sensors such as MEMS devices and energy harvesters, study of different aspects of oscillating structures in microelectronics (both solid-state CMOS oscillators and MEMS oscillators), and investigation and modeling of nonlinear phenomena emerging in such systems. He is an active member of the Technical Committee Nonlinear Circuits and Systems of IEEE CAS society.

Francesco Cottone
Université Paris-Est, ESYCOM, ESIEE Paris, Noisy-le-Grand, France
f.cottone@esiee.fr

Francesco Cottone is a senior researcher and professor at Department of Physics and Geology, University of Perugia, Italy, were he obtained a Ph.D in Physics in 2008. After his Ph.D, Francesco worked outside Italy on nonlinear dynamical systems for vibration energy harvesting at Stokes Institute, University of Limerick, Ireland. In 2011, Francesco awarded a Marie Curie European Fellowship for a project related to nonlinear electrostatic MEMS energy harvesting technology at ESIEE Paris, Université de Paris-Est, France. Since 2013, Francesco re-joined the Noise in Physical System Laboratory, Italy, where he is currently working on nonlinear micro systems and innovative electro-active materials for energy harvesting. His scientific expertise includes gravitational waves detectors, nonlinear stochastic systems and electro-active materials for energy harvesting. He has record of more than 50 referred publications, holds 2 patents and several talks at international conferences on energy harvesting technology.

Einar Halvorsen
University of South-Eastern Norway, Horten, Norway
Einar.Halvorsen@usn.no

Einar Halvorsen received the Siv.Ing. degree in physical electronics from the Norwegian Institute of Technology (NTH), Trondheim, Norway, in 1991, and the Dr.Ing. degree in physics from the Norwegian University of Science and Technology (NTNU, formerly NTH), Trondheim, Norway, in 1996. He has worked both in academia and the microelectronics industry. Since 2004, he has been with University College of Southeast Norway in Horten, Norway, where he is a professor of micro- and nanotechnology. His main research interest is in theory, design, and modelling of microelectromechanical devices.

S. Duy Nguyen
University of South-Eastern Norway, Horten, Norway
Duy.S.Nguyen@hive.no

Son Duy Nguyen received the B.E., and M.E. degrees in electronics from the Ho Chi Minh City University of Technology, Ho Chi Minh City, Vietnam, in 2004 and 2006, respectively, and Ph.D. degree in Applied Micro- and Nanosytems, from the University of Oslo, Norway, in 2013. He was the postdoctoral researcher at Berkeley Sensor & Actuator Center (BSAC), University of California, Berkeley, USA from 2013 to 2015 and 2017. Since 2017, he has been the New Technology Engineer at Analog Devices Inc., USA, where he is the project manager and process development for MEMS devices and biosensors.

Fehmi Najar
LASMAP,Tunisia Polytechnic School, University of Carthage, La Marsa, Tunisia
fehmi.najar@ept.rnu.tn

Fehmi Najar, is Associate Professor of Mechanical Engineering at the Tunisia Polytechnic School, University of Carthage, Tunisia. He received an Engineering Diploma in Mechanical Engineering from the National Engineering School of Tunis in 1997, and an M.S. in Structural Dynamics from the Ecole Centrale de Paris, France, in 1998. After graduation, he worked as Technical Manager in the Graphic Art industry for a period of 6 years. He obtained his PhD in Mechanical Engineering from the National Engineering School of Tunis in 2008. His research interests include MEMS and NEMS, structural dynamics, smart materials, energy harvesting, structural health monitoring, and multi-body dynamics.

Tarik Bourouina
Université Paris-Est, ESYCOM, ESIEE Paris, Noisy-le-Grand, France
t.bourouina@esiee.fr

Tarik Bourouina was born in 1967. He holds a Master of Science (Physics), a Master of Engineering (Electronics) and the Ph.D. degree, obtained in 1991 at Université Paris XII. His entire career was devoted to the field of MEMS. He started research at ESIEE Paris in 1988 among the pioneers in MEMS-based silicon microphones, which he extended to acoustic-based gyroscopes. He then had sev-

eral significant contributions in the area of optical MEMS, among which the smallest MEMS-based FTIR Optical Spectrometer, jointly developed with Si-Ware-System and Hamamatsu Photonics. Among his contributions to the scientific community, he served in the Technical Program Committee of the IEEE MEMS conference (2012, 2013) and joined the Editorial Board of Nature Publishing Group for the journals *Light: Science and Applications* and *Microsystems & Nanoengineering*. Dr. Bourouina took several academic positions in France and in Japan, at the Université Paris-Sud Orsay, at the French National Center for Scientific Research (CNRS) and at The University of Tokyo. Dr. Bourouina is now full Professor at ESIEE Paris, Université Paris-Est since 2002. His current interests include optofluidics and analytical chemistry on-chip, seeking new opportunities for MEMS in the areas of Sustainable Environment and Smart-Cities.